



Cite this: *RSC Adv.*, 2017, 7, 55051

Ligand steric effects on α -diimine nickel catalyzed ethylene and 1-hexene polymerization†

Jinlong Sun,^a Fuzhou Wang,^b  Weimin Li^a and Min Chen^{*a}

A series of *ortho*-dibenzhydryl or *ortho-sec*-phenethyl substituted α -diimine nickel complexes with systematically varied ligand steric effects were used as precatalysts for the polymerization of ethylene and 1-hexene upon activation with Et₂AlCl. The effects of ligand sterics and polymerization temperature on the catalytic activity, molecular weight and polymer microstructure were evaluated in detail. In ethylene polymerization, it is possible to tune the catalytic activities [(0.98–2.41) × 10⁶ g (mol Ni h)⁻¹], polymer molecular weights [M_n : (1.8–13.1) × 10⁵ g mol⁻¹] and branching densities (55–108/1000C) over a very wide range. The molecular weights and branching structure depended on the nickel complexes as well as the polymerization temperature, and the polymer branching densities were decreased with increasing ligand steric effects and decreasing polymerization temperature. Polymerization of 1-hexene with *ortho*-dibenzhydryl substituted nickel complexes resulted in branched polymers (106–140/1000C) with high molecular weights [M_n : (0.64–3.88) × 10⁴ g mol⁻¹] and narrow molecular weight distribution ($M_w/M_n = 1.16$ –1.52, 40–80 °C). The increasing steric hindrance of the catalyst leads to enhanced 2,1-insertion of 1-hexene and the chain-walking reaction.

Received 25th October 2017
 Accepted 28th November 2017

DOI: 10.1039/c7ra11783c

rsc.li/rsc-advances

Introduction

The research on ethylene and α -olefin polymerizations catalyzed by late-transition metal catalysts has been a great highlight for the development of polyolefin materials in recent years.^{1,2} The nickel and palladium complexes ligated by α -diimine^{3,4} showed good activity for ethylene and α -olefin polymerizations to produce a variety of branched polyolefins, because the metal-alkyl species can move on the polymer backbone before the next monomer insertion, *i.e.*, chain-walking,⁵ *via* rapid β -hydride elimination and re-insertion (Scheme 1). Chain-walking polymerization can give polymers with unique structures which cannot be obtained by common vinyl polymerization.^{6,7} The mechanism of chain-walking for α -olefin polymerization involves 1,2- and 2,1-insertion followed by chain-walking (Scheme 1(ii–iv)), in which the active metal center undergoes chain-walking to the terminal carbon followed by monomer insertion.⁸ 1,2-Insertion gives the methyl branch (iii) in a ω ,2-enchainment, while 2,1-insertion gives

a long methylene sequence in a ω ,1-enchainment (iv). If the metal fails to chain walk after 1,2-insertion, the final polymer contains *n*-alkyl branches (ii), which is found in common poly(α -olefin)s. The highly-branched polymers with high amounts of methyl and alkyl branches are amorphous, while the chain-straightened polymers will be semi-crystalline.⁶

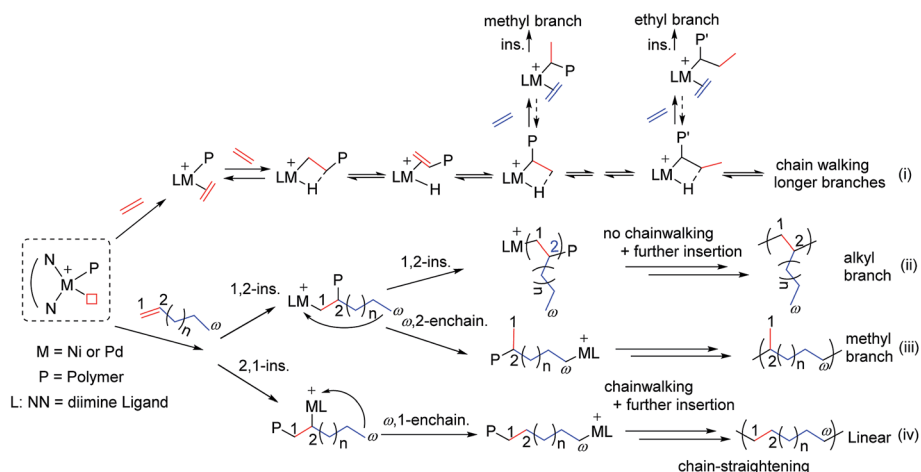
Previous studies indicated that sterically bulky ligands are usually required to afford nickel and palladium catalysts capable of generating high molecular weight polymers.^{2c} Chain straightening polymerization of α -olefins can generate highly linear polyethylene, which is the most abundantly produced plastic owing to its inexpensive monomer, thermoplastic properties, and semi-crystalline nature.^{4d,8} The branching degree of the polymer can be controlled *via* catalyst structures (Chart 1) and polymerization conditions such as ethylene pressures or polymerization temperatures.^{9,10} For example, Wu *et al.* synthesized a camphyl-based α -diimine nickel catalyst **C1** that can polymerize ethylene, propylene and α -olefins in a living fashion under the optimized conditions.¹¹ This catalyst exhibited 1,3-enchainment fraction of 45% in propylene polymerization, and produced poly(α -olefin)s with an obvious T_m . Brookhart *et al.* reported a “sandwich” (8-*p*-tolyl naphthyl) substituted α -diimine nickel catalyst **C2** that yielded highly-branched (up to 152 branches/1000C) polyethylene.¹² Coates *et al.* reported that the living/controlled polymerization of propylene and higher α -olefins using C_2 -symmetric α -diimine nickel catalyst **C3a** bearing chiral *sec*-phenethyl moiety.¹³ Recently, the same group synthesized a dibenzobarrelene-bridged α -diimine nickel catalyst **C3b** bearing chiral *sec*-

^aAdvanced Catalysis and Green Manufacturing Collaborative Innovation Center, School of Petrochemical Engineering, Changzhou University, Changzhou 213164, China. E-mail: wangfuzhou1718@126.com; misschen@ustc.edu.cn

^bGraduate School of Engineering, Hiroshima University, Kagamiyama 1-4-1, Higashi-Hiroshima 739-8527, Japan

† Electronic supplementary information (ESI) available: NMR spectra of ligands and polymers; GPC curves of polymers. CCDC 1576125, 1576349, 1468457 contain the supplementary X-ray crystallographic data for complexes 2, 3 and 5. For ESI and crystallographic data in CIF or other electronic format see DOI: 10.1039/c7ra11783c





Scheme 1 Chain-walking mechanism for ethylene and α -olefin polymerization catalyzed by α -diimine nickel and palladium complexes.

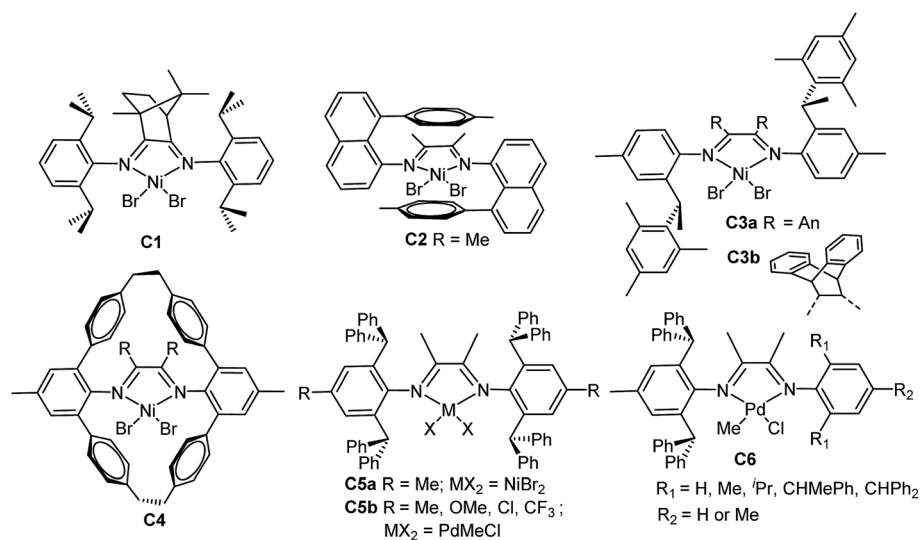


Chart 1 Selected examples of α -diimine nickel and palladium catalysts.

phenethyl moiety.^{4d} The catalyst afforded high molecular weight polyethylenes with narrow dispersities and low degrees of branching, and demonstrated living behavior at room temperature and produced linear polyethylene ($T_m = 135^\circ\text{C}$) at -20°C . Guan *et al.* designed a α -diimine nickel catalyst C4 bearing a macrocyclic ligand, which showed significantly higher thermal stability than the acyclic analogs, and promoted living polymerization of propylene even at 50 – 75°C .¹⁴ This type of catalyst enhances both the 2,1-insertion of propylene and the chain-walking reaction. Long *et al.* examined α -diimine nickel catalysts C5a containing *ortho*-dibenzhydryl moiety for high-temperature ethylene polymerization,¹⁵ where the catalyst maintained high activities at temperatures as high as 100°C .

Chen *et al.* recently reported that α -diimine palladium catalysts C5b bearing the dibenzhydryl moiety displayed high thermal stability and high activity in slow chain-walking ethylene (co)polymerization,¹⁶ producing semicrystalline polyethylene and ethylene/methyl acrylate copolymer with high

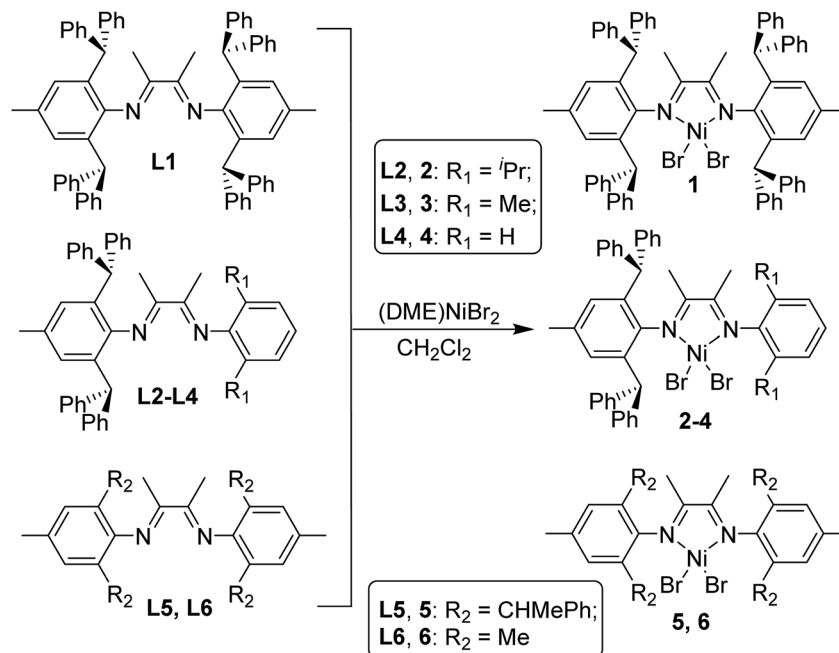
molecular weight and low branching density. They also designed a series of α -diimine palladium catalysts C6 bearing both the dibenzhydryl moiety and with systematically varied ligand sterics for ethylene and 1-hexene polymerization,¹⁷ the molecular weights and branching densities could be tuned over a very wide range. In this work, we wish to report the synthesis of a series of *ortho*-dibenzhydryl and *ortho-sec*-phenethyl substituted α -diimine nickel complexes with systematically varied ligand sterics, and the investigation of the influence of ligand structure and polymerization conditions on ethylene and 1-hexene polymerizations.

Results and discussion

Synthesis and characterization of the nickel complexes

The desired ligands were prepared using the literature procedure in high yields without using column chromatography.^{17,18} α -Diimine nickel precatalysts used in this study are summarized





Scheme 2 Synthesis of α -diimine nickel complexes 1–6.

in Scheme 2. Complexes 2–4 were synthesized from the reactions of the corresponding ligand with (DME)NiBr₂ in high yields. Chen *et al.* previously reported *ortho*-dibenzhydryl and *ortho-sec*-phenethyl substituted nickel complexes **1**^{4f} and **5**¹⁸ that exhibited high activities in ethylene polymerization and produced different branched polyethylene with high molecular weight. Complexes **1** and **5** were prepared and studied in order to obtain accurate comparisons in ethylene polymerization. This way, a series of α -diimine nickel complexes bearing *ortho*-dibenzhydryl and *ortho-sec*-phenethyl groups and with systematically varied ligand sterics could be studied in the polymerization of ethylene and 1-hexene. In addition, the methyl substituted complex **6** was also used for comparison in this study.

X-ray crystallographic studies

Suitable crystals of complexes **2**, **3** and **5** were obtained by layering *n*-hexane onto their dichloromethane solution at room temperature, respectively. The molecular structures of **2**, **3** and **5** was confirmed by single-crystal X-ray diffraction and the corresponding ORTEP diagram with selected bond distances and angles are shown in Fig. 1, 2 and 3, respectively. Crystal data, data collection and refinement parameters are listed in Table S1 (see ESI[†]).

Both unsymmetrical α -diimine nickel complexes **2** (Fig. 1) and **3** (Fig. 2) bearing *ortho*-dibenzhydryl moiety exhibited similar geometries, and a distorted tetrahedron geometry was observed for the Ni center. However, complex **5** (Fig. 3) bearing *ortho-sec*-phenethyl groups exhibited symmetrical chiral pocket about the Ni center, and exhibited near C₂-symmetry. In the solid state, the most interesting feature of ligand is the conformation of the substituents attached to N1 and N2. These

groups are rotated about 180° from the position they must occupy to chelate metal Ni. The rotation has been confirmed by the crystal structure of its complex. The X-ray structures of ligand¹⁸ and complex exhibit *trans* and *cis* conformation about the central C–C bond of the backbone, respectively. Both aryl

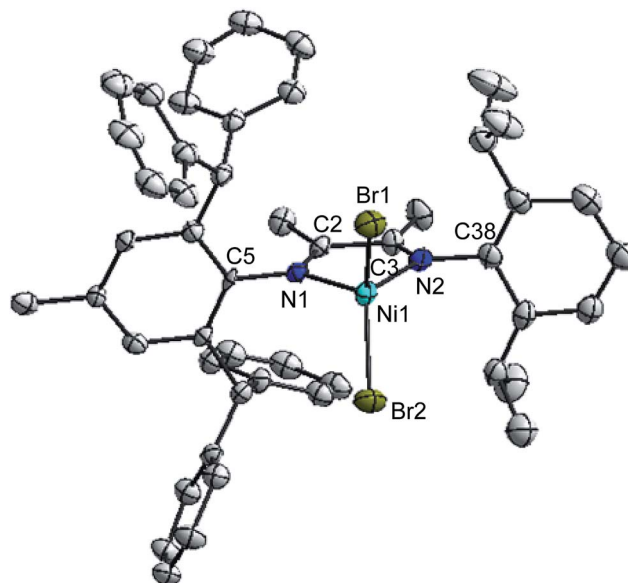


Fig. 1 Molecular structure of complex **2** with thermal ellipsoids drawn at 30% probability, and H atoms have been omitted for clarity. Selected bond lengths (Å) and angles (°): Ni1–N1 = 2.018(13), Ni1–N2 = 2.026(13), Ni1–Br1 = 2.331(3), Ni1–Br2 = 2.334(3), N1–C2 = 1.27(2), N1–C5 = 1.43(2); N1–Ni1–N2 = 80.4(5), N1–Ni1–Br1 = 114.3(4), N2–Ni1–Br1, 110.0(5), N1–Ni1–Br2 = 111.8(4), N2–Ni1–Br2 = 118.2(4), Br1–Ni1–Br2 = 116.90(13), C2–N1–Ni1 = 111.6(11), C5–N1–Ni1 = 128.7(10).



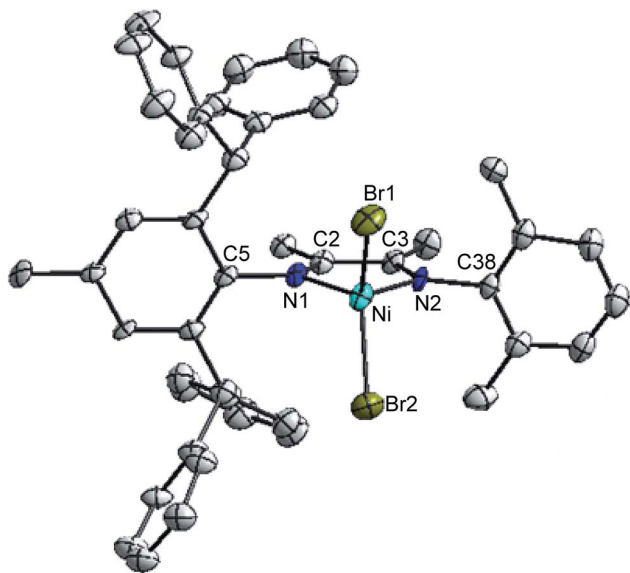


Fig. 2 Molecular structure of complex 3 with thermal ellipsoids drawn at 30% probability, and H atoms have been omitted for clarity. Selected bond lengths (Å) and angles (°): Ni1–N1 = 2.018(13), Ni1–N2 = 2.026(13), Ni1–Br1 = 2.331(3), Ni1–Br2 = 2.334(3), N1–C2 = 1.27(2), N1–C5 = 1.43(2), N2–C3 = 1.17(2), N2–C38 = 1.48(2), C2–C3 = 1.53(2), N1–Ni1–N2 = 80.4(5), N1–Ni1–Br1 = 114.3(4), N2–Ni1–Br1 = 110.0(5), N1–Ni1–Br2 = 111.8(4), N2–Ni1–Br2 = 118.2(4), Br1–Ni1–Br2 = 116.90(13), C2–N1–C5 = 119.4(14), C2–N1–Ni1 = 111.6(11), C5–N1–Ni1 = 128.7(10), C3–N2–C38 = 121.4(16), C3–N2–Ni1 = 115.4(13), C38–N2–Ni1 = 123.2(11).

rings bonded to the imine nitrogen of the α -diimine lie nearly perpendicular to the plane formed by the nickel and coordinated nitrogen atoms. The bond angles and bond distances are consistent with those previously reported for α -diimine nickel complexes.⁴ In fact, the Ni1–N1 bond distances in complex 2 (2.026 Å) and 3 (2.018 Å) are similar to these in 5 (2.034 Å), as well as the Ni1–Br1 bond distances (2.331 Å for 2; 2.331 Å for 3; 2.3308 Å for 5). In addition, the Br1–Ni1–Br2 angles are 116.90° for complex 2 and 116.90° for complex 3 are similar to these in complex 5 (117.30°).

Ethylene polymerization studies

All the dibromo nickel complexes 1–6 were applied to ethylene polymerization activated by Et₂AlCl at the [Al]/[Ni] molar ratio of 600 for 30 min under 9 atm of ethylene (Table 1). First, the influence of the polymerization temperature was studied by varying the temperature from 20 to 80 °C. The catalytic activities of complex 1 were increased with polymerization temperatures and the highest activity was observed at 80 °C (entry 3, Table 1). The maximum catalytic activities for complexes 2–5 were observed at 50 °C (entries 5, 8, 11 and 14, Table 1), and the polymerization at 80 °C still gave high catalytic activities on the level of 10⁶ g of PE per (mol Ni h) (entries 6, 9, 12 and 15, Table 1). Therefore, these α -diimine nickel complexes 1–5 were highly active in ethylene polymerization, and showed much higher thermal stability than the corresponding methyl substituted complex 6.

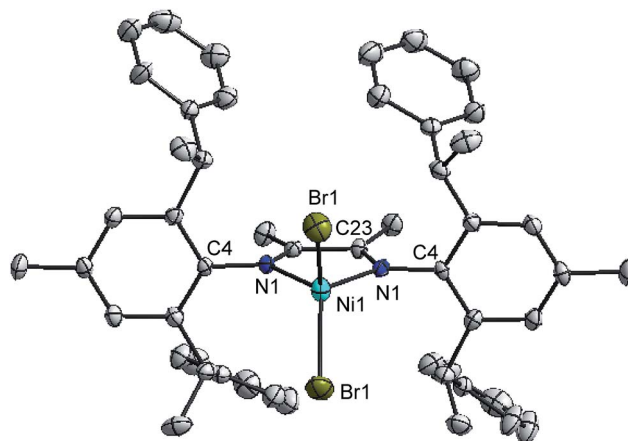


Fig. 3 Molecular structure of complex 5 with thermal ellipsoids drawn at 30% probability, and H atoms have been omitted for clarity. Selected bond lengths (Å) and angles (°): Br1–Ni1 = 2.3308(12), Br1i–Ni1 = 2.3309(12), Ni1–N1 = 2.034(5), N1–C4 = 1.421(7), N1–C23 = 1.297(8), C23–C23i = 1.514(11); Br1–Ni1–Br1i = 117.30(9), Ni1–Ni1–N1 = 81.2(3), Ni1–Ni1–Br1 = 112.14(14), N1–Ni1–Br1 = 114.40(14), N1–Ni1–Br1i = 112.14(14), Ni1–Ni1–Br1i, 114.40(14), C4–N1–Ni1, 124.5(4).

On the other hand, the polymer molecular weight was strongly depended on the polymerization temperature with narrow molecular weight distributions of $M_w/M_n \leq 2.50$. The maximum molecular weight was observed at 50 °C (entries 2, 5, 8, 11 and 14, Table 1). Further increase of temperature caused a decrease in the molecular weight accompanied by broadening of the molecular weight distribution (entries 3, 6, 9, 12 and 15, Table 1). This suggests that fast chain transfer takes place at higher temperatures.¹⁴

Then, the effect of catalyst precursors 1–6 were investigated with [Al]/[Ni] ratio of 600 (entries 1–18, Table 1). Complexes 1–5 produced polymers in high yields with high molecular weights ($M_n \geq 1.8 \times 10^5$ g mol⁻¹) and narrow molecular weight distributions ($M_w/M_n = 1.50$ –2.50). Steric effect of *ortho*-position in the anilinic moiety can be evaluated by comparing 1 to 4 and 5, 6. At 50 °C and 9 atm of ethylene pressure, the polymerization activity decreased in the following order, 2 \geq 3 \geq 4 \geq 5 \geq 1 > 6 (entries 2, 5, 8, 11, 14 and 17, Table 1).

Complex 2 with isopropyl groups showed the highest activity among these complexes, but gave the lower molecular weight than that of complex 1. At 50 °C, the molecular weight of the polymers decreased in the following order, 1 \geq 5 \geq 2 \geq 3 \geq 4 \geq 6. These results indicated that the rate of chain propagation was greatly promoted by the bulky *ortho*-dibenzhydryl and *ortho*-*sec*-phenethyl substituents of the ligand's aryl rings. The highest molecular weight of the polymer obtained by complex 1 suggests that the bulky *ortho*-dibenzhydryl could efficiently suppress chain-transfer reactions.

The branching densities of the obtained polyethylenes were determined by ¹H NMR spectroscopy,¹⁹ and the results are shown in Table 1. The branching densities were increased with polymerization temperature from 20 to 80 °C (1, 55–64/1000C; 2, 81–90/1000C; 3, 86–98/1000C; 4, 95–108/1000C; 5, 87–103/1000C; 6, 90–95/1000C). The branching densities were



Table 1 Effect of catalyst and temperature on ethylene polymerization^a

Entry	Precat.	Temp (°C)	Yield (g)	Activity ^b	M_n^c	M_w/M_n^c	B^d
1	1	20	1.18	0.98	9.9	1.80	55
2	1	50	1.69	1.41	13.1	1.99	58
3	1	80	1.89	1.58	8.0	1.69	64
4	2	20	2.21	1.84	7.2	1.62	81
5	2	50	2.89	2.41	8.1	1.50	84
6	2	80	2.59	2.16	5.2	2.13	90
7	3	20	1.75	1.46	4.0	2.09	86
8	3	50	2.85	2.38	6.5	2.06	91
9	3	80	2.09	1.74	2.9	2.19	98
10	4	20	2.11	1.76	2.2	1.96	95
11	4	50	2.76	2.30	2.9	2.32	101
12	4	80	1.78	1.48	1.8	2.50	108
13	5	20	2.13	1.78	7.3	1.52	87
14	5	50	2.65	2.21	8.7	1.80	93
15	5	80	1.84	1.53	5.4	2.09	103
16	6	20	0.76	0.63	0.8	1.67	90
17	6	50	0.53	0.44	0.6	1.98	95
18	6	80	Trace	—	—	—	—

^a Polymerization conditions: Ni = 2.4 μmol in CH_2Cl_2 (2 mL); cocatalyst Et_2AlCl , Al/Ni = 600; toluene = 20 mL; 9 atm of ethylene; time = 30 min. ^b 10^6 g of PE (mol of Ni)⁻¹ h⁻¹. ^c M_n and M_w/M_n determined by GPC, 10^5 g mol⁻¹. ^d Branching numbers per 1000C were determined by ¹H NMR.

decreased by increasing the steric bulkiness of the *ortho* substituents on the α -diimine ligands by comparing **1** to **4**. For example, at 50 °C, the number of chain branching was depended on the precatalysts and decreased in the following order, **4** [2,6-di(*H*), 101/1000C] > **3** [2,6-di(Me), 91/1000C] > **2** [2,6-di(^{*i*}Pr), 84/1000C] > **1** [2,6-di(CHPh₂), 58/1000C] (entries 2, 5, 8 and 11, Table 1). These results indicated that the introduction of dibenzhydryl substituent into the *ortho*-position of the imines ligands can decrease the branching degree of the polyethylenes.^{15,16} In addition, complex **5** [2,6-di(CHMePh), 50 °C, 93/1000C] led to slightly lower branching density than complex **6** [2,6-di(Me), 50 °C, 95/1000C].

The branching structures analysis based on ¹³C NMR showed that 74 methyl, 7 ethyl, 5*n*-propyl, 4*n*-butyl, 1-*sec*-butyl (branch on branch structure) and 17 longer chains (>C4 branches) exist for the polyethylene produced by complex **4** at 80 °C (Fig. 4(i), entry 12, Table 1). In contrast, only 55 methyl branches were observed for complex **1** at 20 °C (Fig. 4(ii), entry 1, Table 1). The microstructure difference and the lower degree of branching density for the sterically bulkier catalysts are probably due to the relatively greater preference of insertion of ethylene into a primary metal alkyl species *versus* insertion into a secondary metal-alkyl species.¹⁶ The rationale for the formation of the major types of branches (methyl, ethyl, propyl, butyl and longer chains) in the polyethylenes obtained in this work is shown in Scheme 1(i).

1-Hexene polymerization studies

Chen *et al.* recently reported the tuning of polyethylene and poly(1-hexene) microstructures using a series of α -diimine palladium complexes **C6** bearing both the dibenzhydryl moiety

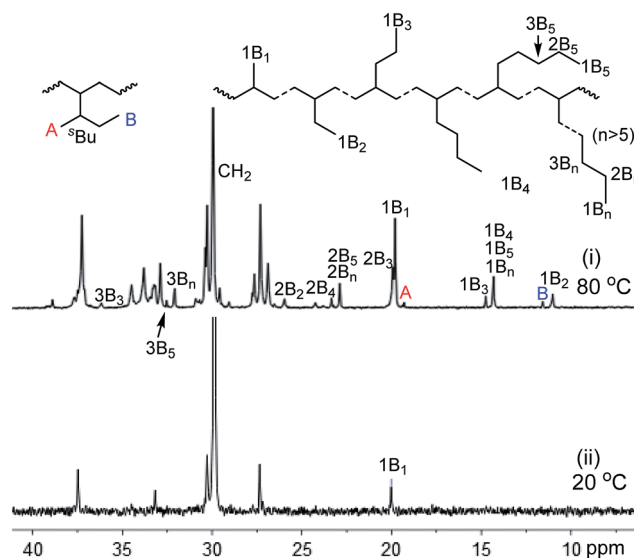


Fig. 4 ¹³C NMR spectra of polyethylenes obtained by complex **1** at 20 °C (ii) and complex **4** at 80 °C (i) (A and B refer to methyl carbon of *sec*-butyl branches, entries 1 and 12, Table 1).

and with systematically varied ligand sterics.¹⁷ In the above-mentioned ethylene polymerization, a series of α -diimine dibenzhydryl substituted nickel complexes **1–4** with systematically varied ligand sterics showed high activities and high thermal stability, and produced polyethylene with high molecular weight. The tuning in ligand sterics enables the tuning of the polymer microstructures such as molecular weight and branching density. Therefore, polymerization of 1-hexene using these complexes **1–4** activated by Et_2AlCl were carried out at various polymerization temperatures (20–80 °C) with the [Al]/[Ni] ratio of 500, and the results are listed in Table 2. In comparison with polymerization of ethylene, a decrease in catalytic activity was observed, which is due to the steric bulkiness of the 1-hexene monomer. The lowest catalytic activity was observed for **1** among these complexes, because bulky steric hindrance of complex **1** is unfavorable for 1-hexene monomer insertion, especially at lower temperature (no polymer was obtained at 20 °C, entry 1, Table 2).

As shown in Table 2, both the catalytic activities of complexes **1**, **3** and the molecular weight of the obtained polymers were slightly increased with polymerization temperatures (entries 1–4 and 9–12), but the opposite trend was observed for complexes **2** and **4** (entries 6–8 and 13–16). Complex **2** showed the highest polymer molecular weight ($M_n = 3.88 \times 10^5$ g mol⁻¹, entry 6, Table 2) at 40 °C among these catalysts. Complexes **2** and **3** showed good activity for 1-hexene polymerization to produce polymers with high molecular weight and narrow molecular weight distribution ($M_w/M_n = 1.16–1.32$, entries 6–12, Table 2), indicating the living characteristics of the polymerizations.

Generally, polymer microstructure is strongly dependent on catalyst structure and polymerization temperature. The branching structures of the poly(1-hexene)s produced by α -diimine nickel complexes **1–4** were determined and analyzed to



Table 2 Polymerization of 1-hexene by α -diimine nickel complexes 1–4^a

Entry	Precat.	Temp (°C)	Yield (g)	Act. ^b	M_n^c	M_w/M_n^c	B^d	Mol fraction of C6 unit (χ) ^d		
								Linear (χ_L)	Methyl-branched (χ_M)	Alkyl-branched (χ_A)
1	1	20	Trace	—	—	—	—	—	—	—
2	1	40	0.03	0.10	0.66	1.16	111.3	0.332	0.526	0.142
3	1	60	0.11	0.37	1.22	1.20	106.7	0.360	0.521	0.119
4	1	80	0.16	0.53	1.63	1.28	105.9	0.365	0.519	0.116
5	2	20	0.84	2.80	3.16	2.14	118.6	0.289	0.428	0.283
6	2	40	0.79	2.63	3.88	1.29	119.0	0.286	0.492	0.222
7	2	60	0.65	2.17	1.17	1.32	121.6	0.271	0.565	0.164
8	2	80	0.40	1.33	0.80	1.32	123.0	0.262	0.590	0.148
9	3	20	0.46	1.53	1.67	1.16	124.5	0.253	0.427	0.320
10	3	40	0.75	2.50	2.06	1.25	118.1	0.292	0.460	0.248
11	3	60	0.82	2.73	3.39	1.31	118.7	0.288	0.523	0.189
12	3	80	0.83	2.77	3.51	1.23	119.0	0.286	0.558	0.156
13	4	20	1.10	3.67	—	—	—	—	—	—
14	4	40	0.64	2.13	1.83	1.51	134.6	0.193	0.585	0.222
15	4	60	0.54	1.80	1.12	1.52	138.9	0.167	0.613	0.220
16	4	80	0.25	0.83	0.64	1.33	140.0	0.160	0.631	0.209

^a Polymerization conditions: Ni = 10 μ mol in CH_2Cl_2 (2 mL); cocatalyst Et_2AlCl , Al/Ni = 500; monomer concentration [1-hexene] = 1 M; time: t = 3 h; solvent: toluene, total volume: 20 mL. ^b Activity in 10^4 g (mol Ni)⁻¹ h⁻¹. ^c M_n and M_w/M_n determined by GPC, 10^5 g mol⁻¹. ^d Determined using ¹H NMR spectroscopy.⁸

study the relationship between polymer microstructure and catalyst structure.

¹H NMR spectroscopy analyses have shown that the branching degree of the obtained poly(1-hexene)s are lower than the theoretical value (166.7/1000C) due to the 2,1-insertion of 1-hexene and the 1,6-enchainment (Scheme 1(iv)). The branching degree could be only tuned over a narrow range (106–140/1000C, Table 2) comparing with that in ethylene polymerization. For example, the branching densities (106–111/1000C, entries 2–4, Table 2) of the polymers obtained by complex 1 decreased with increasing temperature, but complex 4 increased slightly (135–140/1000C, entries 14–16, Table 2). However, the branching densities of the obtained polymers by complexes 2 and 3 are very close to 120 branches per 1000C, and are not depend on the polymerization temperature (entries 5–12, Table 2).

Polymers were analyzed by quantitative NMR spectroscopy to obtain the mole fractions of the three major C6 units: linear

(χ_L), methyl-branched (χ_M), and alkyl-branched (χ_A) (see ESI† for details).⁸ The highly branched polymers with methyl and alkyl branches will be amorphous, while the chain-straightened (χ_L) polymers will be semi-crystalline. As shown in the polymer microstructures by complexes 1 and 2, the mole fractions of the three major C6 units decreased in the following order, $\chi_M > \chi_L \geq \chi_A$. The increasing steric hindrance of catalyst leads to enhanced insertion for 2,1-insertion of 1-hexene (χ_L : 1 > 2 \approx 3 > 4) and the chain-walking reaction. This indicated that the steric hindrance of *ortho*-dibenzhydryl substituent on catalysts could suppress chain-transfer reactions (Fig. 5). The predominance of methyl branch ($\chi_M = 0.43$ –0.63) means that the predominate 1,2-insertion followed by chain-walking forms a 2, ω -enchainment (Scheme 1(iii)).

In addition, the polymerization temperature also influences the branch-type distribution. The mole fraction of linear enchainment (χ_L) of the obtained amorphous polymers (no T_m observed) by complexes 1 and 3 slightly increased from 0.33 to 0.37 and 0.25 to 0.29 with increasing temperatures, while χ_A slightly decreased to 0.12 and 0.16 (entries 2–4 and 9–12, Table 2). The use of the complexes 2 and 4 result in a considerable decline in χ_L with increasing temperature (entries 5–8 and 14–16, Table 2), and the obtained polymers were amorphous.

Conclusion

In summary, polymerizations of ethylene and 1-hexene were catalyzed using a series of α -diimine nickel complexes bearing *ortho*-dibenzhydryl or *ortho-sec*-phenethyl groups activated by Et_2AlCl . The ligands were modified in an attempt to change the coordination environment, steric effects and the electronic density of the metal center, eventually to modulate the activity in the polymerization of ethylene/1-hexene and to control the

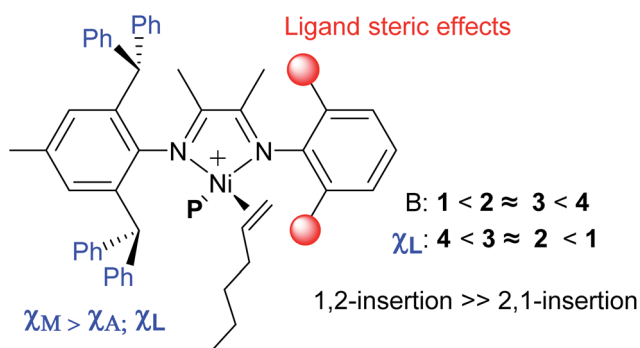


Fig. 5 Ligand steric effects of the 1-hexene insertion for α -diimine nickel complexes 1–4.



microstructure of polymers. The polymerization results indicated the possibility of precise microstructure control, depending on the catalyst structure and polymerization temperature, which in turn strongly affects the physical properties. The sterically bulky complex showed higher catalytic activities and thermal stability in ethylene polymerization and produced polyethylene with high molecular weight and much lower polyethylene branching density. The polyethylene branching densities (55–108/1000C) were decreased with increasing the bulkiness of the ligand and decreasing the polymerization temperature. However, sterically bulky complex is unfavorable for 1-hexene monomer insertion, and leads to low catalytic activity in 1-hexene polymerization.

Experimental section

General considerations

All experiments were carried out under a dry N₂ atmosphere by using standard Schlenk techniques or a glovebox. Research grade ethylene was purified by passing it through an Agilent oxygen/moisture trap. ¹H and ¹³C NMR spectra were recorded with a Bruker Ascend 400 spectrometer at ambient temperature unless otherwise stated. The chemical shifts of the ¹H and ¹³C NMR spectra were referenced to tetramethylsilane (TMS). The molecular weight and the molecular weight distribution of the polymers were determined by gel permeation chromatography (GPC, Toshi, Tokyo, Japan) equipped with two linear Styragel columns at 40 °C using THF as a solvent and calibrated with polystyrene standards, and THF was employed as the eluent at a flow rate of 0.35 mL min⁻¹. Elemental analysis was performed by the Analytical Center of the University of Science and Technology of China. Mass spectra were recorded on a P-SIMS-Gly from Bruker Daltonics Inc (EI⁺). 1-Hexene was purchased from Kanto Chemical Co on Aldrich Chemical Company were dried over CaH₂, and distilled before use. Dichloromethane, toluene, THF, and hexane were purified by solvent purification systems. α -Diimine ligands L1–6^{17,18} and complexes 1,^{4f,15a} 5,¹⁸ 6¹⁸ were prepared according to reported procedures. Other chemicals were commercially obtained and purified with common procedures.

Synthesis of complexes 2–4

All complexes were prepared in a similar manner by the reaction of (DME)NiBr₂ (DME = 1,2-dimethoxyethane) with the corresponding ligands in dichloromethane. A typical synthetic procedure of 2–4 is as follows: (DME)NiBr₂ (0.31 g, 1.0 mmol) and ligand¹⁷ (1.0 mmol) were combined in a Schlenk flask under a N₂ atmosphere. CH₂Cl₂ (20 mL) was added, and the reaction mixture was stirred at room temperature for 12 h. The resulting suspension was filtered. The solvent was removed under vacuum, and the resulting powder was washed with diethyl ether (2 × 10 mL), and then dried under vacuum at room temperature to obtain a brown solid powder.

(¹⁵N¹⁵N)NiBr₂ (2). (0.75 g, 93%): anal. calcd for (C₄₉H₅₀Br₂N₂Ni): C, 66.47; H, 5.69; N, 3.16. Found: C, 66.79; H, 5.60; N,

3.45. MALDI-TOF-MS (*m/z*): calcd for C₄₉H₅₀BrN₂Ni: 803.2511, found: 803.1885 [M – Br]⁺.

(¹³C¹³N¹³N)NiBr₂ (3). (0.71 g, 95%): anal. calcd for (C₄₅H₄₂Br₂N₂Ni): C, 65.17; H, 5.10; N, 3.38. Found: C, 65.49; H, 5.42; N,

3.41. MALDI-TOF-MS (*m/z*): calcd for C₄₅H₄₂BrN₂Ni: 747.1885, found: 747.1255 [M – Br]⁺.

(¹³C¹³N¹³N)NiBr₂ (4). (0.66 g, 92%): anal. calcd for (C₄₃H₃₈Br₂N₂Ni): C, 64.45; H, 4.78; N, 3.50. Found: C, 64.49; H, 4.52; N,

3.45. MALDI-TOF-MS (*m/z*): calcd for C₄₃H₃₈BrN₂Ni: 719.1572, found: 719.1244 [M – Br]⁺.

X-ray structure determinations

Single crystals of complexes 2, 3 and 5 for X-ray analysis were obtained by dissolving the nickel complex in CH₂Cl₂, followed by slow layering of the resulting solution with at room temperature. Data collections were performed at 296(2) K on a Bruker SMART APEX diffractometer with a CCD area detector, using graphite monochromated MoK α radiation ($\lambda = 0.71073$ Å). The determination of crystal class and unit cell parameters was carried out by the SMART program package. The raw frame data were processed using SAINT and SADABS to yield the reflection data file. The structures were solved by using the SHELXTL program. Refinement was performed on *F*² anisotropically for all non-hydrogen atoms by the full-matrix least-squares method. The hydrogen atoms were placed at the calculated positions and were included in the structure calculation without further refinement of the parameters. Details of the crystal data and structure refinements for complex 2 are listed in Table S1.†

Procedure for ethylene polymerization

In a typical experiment, a 350 mL glass thick-walled pressure vessel was charged with required amount of AlEt₂Cl, 20 mL toluene and a magnetic stir bar in the glovebox. The pressure vessel was connected to a high pressure polymerization line and the solution was degassed. The vessel was warmed to the desired temperature using an oil bath and allowed to equilibrate for 5 min. Then 2.4 μ mol of nickel complex in 2 mL CH₂Cl₂ was injected into the vessel *via* syringe. With rapid stirring, the reactor was pressurized and maintained at 9.0 atm of ethylene. After the desired amount of polymerization time, the vessel was vented and terminated in acidified methanol (methanol/HCl = 50/1). The polymers obtained were adequately washed with methanol and dried under vacuum at 50 °C for 24 h. Analysis of the polyethylene branching by ¹H NMR spectroscopy: branching density, branches/1000C = (CH₃/3)/[(CH + CH₂ + CH₃)/2] × 1000. CH₃ (alkyl methyl, alk-CH₃, m, 0.70–0.95 ppm), CH₂ and CH (alk-CH and alk-CH₂, m, *ca.* 1.00–1.45 ppm) refer to the intensities of the methyl, methylene and methine resonances in ¹H NMR spectra.¹⁹

Procedure for 1-hexene polymerization

In a typical procedure, a round-bottom Schlenk flask with stirring bar was heated 1 h at 150 °C under vacuum and cooled to room temperature. After drying the reactor under N₂ atmosphere, toluene was added to the reactor. 1-Hexene was added



to the toluene kept at polymerization temperature *via* a syringe. Then the co-catalyst AlEt₂Cl was added to the toluene and the mixture was stirred for 10 min. Polymerization was started by the addition of the catalyst solution (10 μmol, 2 mL CH₂Cl₂) into the reactor *via* syringe, and the total volume of the solution was kept at 20 mL. After the desired amount of time, the polymerization was terminated by adding 50 mL of the acidified methanol (methanol/HCl = 50/1). The polymers obtained were adequately washed with methanol and dried in vacuum at 40 °C to a constant weight. Poly(1-hexene)s show long methylene sequences [linear (χ_L)], methyl branch (χ_M) and alkyl branches [*i.e.*, butyl and longer than hexyl branches (χ_A)].^{46,17} Analysis of the poly(1-hexene) branching by ¹H NMR spectroscopy:⁸ branching density, branches/1000C = (CH₃/3)/[(CH + CH₂ + CH₃)/2] × 1000. CH₃ (alk-CH₃ (χ_M), d, 0.70–0.87 ppm; alkyl methyl (χ_A), t, 0.87–0.95 ppm), CH₂ and CH (alk-CH and alk-CH₂, m, *ca.* 1.0–1.45 ppm) refer to the intensities of the methyl, methylene and methine resonances in ¹H NMR spectra. 2,1-Insertion was calculated by the following equation: 2,1-Ins.% = χ_L = 2,1-insertion = (166.7 - B)/166.7,^{11b,12} B = branches per 1000C; χ_M + χ_A = 1 - χ_L.

Conflicts of interest

There are no conflicts to declare.

Acknowledgements

This work was supported by National Natural Science Foundation of China (NSFC, 21704094), the Chinese Postdoctoral Science Foundation (2017M612076), Advanced Catalysis and Green Manufacturing Collaborative Innovation Center (ACGM2016-06-01) and Yixing Taodu Ying Cai Program.

Notes and references

- (a) S. D. Ittel, L. K. Johnson and M. Brookhart, *Chem. Rev.*, 2000, **100**, 1169–1203; (b) T. R. Younkin, E. F. Connor, J. I. Henderson, S. K. Friedrich, R. H. Grubbs and D. A. Bansleben, *Science*, 2000, **287**, 460–462; (c) J. M. Rose, F. Deplace, N. A. Lynd, Z. Wang, A. Hotta, E. B. Lobkovsky, E. J. Kramer and G. W. Coates, *Macromolecules*, 2008, **41**, 9548–9555; (d) C. Chen, S. Luo and R. F. Jordan, *J. Am. Chem. Soc.*, 2008, **130**, 12892–12893; (e) C. Chen, S. Luo and R. F. Jordan, *J. Am. Chem. Soc.*, 2010, **132**, 5273–5284; (f) D. Zhang and C. L. Chen, *Angew. Chem., Int. Ed.*, 2017, **56**, 14672–14676.
- (a) R. Nakano and K. Nozaki, *J. Am. Chem. Soc.*, 2015, **137**, 10934–10937; (b) X. L. Sui, S. Y. Dai and C. L. Chen, *ACS Catal.*, 2015, **5**, 5932–5937; (c) M. Chen, W. P. Zou, Z. G. Cai and C. L. Chen, *Polym. Chem.*, 2015, **6**, 2669–2676; (d) Y. Ota, S. Ito, M. Kobayashi, S. Kitade, K. Sakata, T. Tayano and K. Nozaki, *Angew. Chem., Int. Ed.*, 2016, **55**, 7505–7509; (e) Z. Jian, L. Falivene, G. Boffa, S. Ortega Sánchez, L. Caporaso, A. Grassi and S. Mecking, *Angew. Chem., Int. Ed.*, 2016, **55**, 14378–14595; (f) B. P. Yang, S. Y. Xiong and C. L. Chen, *Polym. Chem.*, 2017, **8**, 6272–6276; (g) T. Liang and C. L. Chen, *Organometallics*, 2017, **36**, 2338–2344; (h) Y. N. Na, D. Zhang and C. L. Chen, *Polym. Chem.*, 2017, **8**, 2405–2409.
- (a) J. C. Yuan, F. Z. Wang, W. B. Xu, T. J. Mei, J. Li, B. N. Yuan, F. Y. Song and Z. Jia, *Organometallics*, 2013, **32**, 3960–3968; (b) L. Zhu, Z. S. Fu, H. J. Pan, W. Feng, C. L. Chen and Z. Q. Fan, *Dalton Trans.*, 2014, **43**, 2900–2906; (c) W. P. Zou and C. L. Chen, *Organometallics*, 2016, **35**, 1794–1801; (d) R. K. Wang, M. H. Zhao and C. L. Chen, *Polym. Chem.*, 2016, **7**, 3933–3938; (e) S. Yuan, E. Yue, C. Wen and W. H. Sun, *RSC Adv.*, 2016, **6**, 7431–7438; (f) P. Huo, J. Li, W. Liu, G. Mei and X. H. He, *RSC Adv.*, 2017, **7**, 51858–51863; (g) Y. N. Na, X. Wang, K. Lian, Y. Zhu, W. Li, Y. Luo and C. L. Chen, *ChemCatChem*, 2017, **9**, 1062–1066; (h) M. H. Zhao and C. L. Chen, *ACS Catal.*, 2017, **7**, 7490–7494.
- (a) J. C. Yuan, F. Z. Wang, B. N. Yuan, Z. Jia, F. Y. Song and J. Li, *J. Mol. Catal. A: Chem.*, 2013, **370**, 132–139; (b) F. Z. Wang, R. Tanaka, Q. S. Li, J. C. Yuan, Y. Nakayama and T. Shiono, *J. Mol. Catal. A: Chem.*, 2015, **398**, 231–240; (c) L. H. Guo and C. L. Chen, *Sci. China: Chem.*, 2015, **58**, 1663–1673; (d) B. K. Long, J. M. Eagan, M. Mulzer and G. W. Coates, *Angew. Chem., Int. Ed.*, 2016, **55**, 7222–7226; (e) F. Z. Wang, R. Tanaka, Z. G. Cai, Y. Nakayama and T. Shiono, *Polymers*, 2016, **8**, 160; (f) L. H. Guo, S. Y. Dai and C. L. Chen, *Polymers*, 2016, **8**, 37; (g) L. H. Guo, W. Liu and C. L. Chen, *Mater. Chem. Front.*, 2017, **1**, 2487–2494.
- (a) G. Chen, X. S. Ma and Z. Guan, *J. Am. Chem. Soc.*, 2003, **125**, 6697–6704; (b) B. K. Bahuleyan, G. W. Son, D. W. Park, C. S. Ha and I. Kim, *J. Polym. Sci., Part A: Polym. Chem.*, 2008, **46**, 1066–1082; (c) C. Chen and R. F. Jordan, *J. Am. Chem. Soc.*, 2010, **132**, 10254–10255; (d) R. K. Wang, X. L. Sui, W. M. Pang and C. L. Chen, *ChemCatChem*, 2016, **8**, 434–440; (e) M. Li, X. B. Wang, Y. Luo and C. L. Chen, *Angew. Chem., Int. Ed.*, 2017, **129**, 11762–11767.
- (a) E. Yue, L. Zhang, Q. Xing, X. P. Cao, X. Hao, C. Redshaw and W. H. Sun, *Dalton Trans.*, 2014, **43**, 423–431; (b) Y. Ota, S. Ito, J. Kuroda, Y. Okumura and K. Nozaki, *J. Am. Chem. Soc.*, 2014, **136**, 11898–11901; (c) Z. B. Jian, B. C. Moritz and S. Mecking, *J. Am. Chem. Soc.*, 2015, **137**, 2836–2839; (d) L. H. Guo, S. Y. Dai, X. L. Sui and C. L. Chen, *ACS Catal.*, 2016, **6**, 428–441; (e) X. H. Hu, S. Y. Dai and C. L. Chen, *Dalton Trans.*, 2016, **45**, 1496–1503; (f) K. Lian, Y. Zhu, W. Li, S. Y. Dai and C. L. Chen, *Macromolecules*, 2017, **50**, 6074–6080.
- (a) Y. Chen, L. Wang, H. Yu, Y. Zhao, R. Sun, G. Jing, J. Huang, H. Khalid, N. M. Abbasi and M. Akram, *Prog. Polym. Sci.*, 2015, **45**, 23–43; (b) S. Y. Dai, X. L. Sui and C. L. Chen, *Chem. Commun.*, 2016, **52**, 9113–9116; (c) X. L. Sui, C. W. Hong, W. M. Pang and C. L. Chen, *Mater. Chem. Front.*, 2017, **1**, 967; (d) M. Chen and C. L. Chen, *ACS Catal.*, 2017, **7**, 1308–1312.
- (a) T. Vaidya, K. Klimovica, A. M. LaPointe, I. Keresztes, E. B. Lobkovsky, O. Daugulis and G. W. Coates, *J. Am. Chem. Soc.*, 2014, **136**, 7213–7216; (b) F. Z. Wang, S. S. Tian, R. P. Li, W. M. Li and C. L. Chen, *Chin. J. Polym. Sci.*, 2018, **36**, 1–6; (c) C. Y. Rong, F. Z. Wang, W. M. Li and M. Chen, *Organometallics*, 2017, **36**, 4458–4464.



- 9 (a) L. H. Guo, H. Gao, Q. Guan, H. Hu, J. Deng, J. Liu, F. Liu and Q. Wu, *Organometallics*, 2012, **31**, 6054–6062; (b) Q. Mahmood, Y. N. Zeng, X. X. Wang, Y. Sun and W. H. Sun, *J. Organomet. Chem.*, 2015, **798**, 401–407; (c) Q. Mahmood, Y. N. Zeng, X. X. Wang, Y. Sun and W. H. Sun, *Dalton Trans.*, 2017, **46**, 6934–6947.
- 10 (a) S. Kong, K. Song, T. Liang, C. Y. Guo, W. H. Sun and C. Redshaw, *Dalton Trans.*, 2013, **42**, 9176–9187; (b) C. J. Stephenson, J. P. McInnis, C. Chen, M. P. Weberski, A. Motta, M. Delferro and T. J. Marks, *ACS Catal.*, 2014, **4**, 999–1003; (c) H. Hu, H. Gao, D. Chen, G. Li, Y. Tan, G. Liang, F. Zhu and Q. Wu, *ACS Catal.*, 2015, **5**, 122–128; (d) F. Z. Wang, R. Tanaka, Z. G. Cai, Y. Nakayama and T. Shiono, *Macromol. Rapid Commun.*, 2016, **37**, 1375–1381; (e) F. Z. Wang, R. Tanaka, Z. G. Cai, Y. Nakayama and T. Shiono, *Polymer*, 2017, **127**, 88–100.
- 11 (a) F. S. Liu, H. Y. Gao, Z. L. Hu, H. B. Hu, F. M. Zhu and Q. Wu, *J. Polym. Sci., Part A: Polym. Chem.*, 2012, **50**, 3859–3866; (b) J. Liu, D. R. Chen, H. Wu, Z. F. Xiao, H. Y. Gao, F. M. Zhu and Q. Wu, *Macromolecules*, 2014, **47**, 3325–3331.
- 12 D. F. Zhang, E. T. Nadres, M. Brookhart and O. Daugulis, *Organometallics*, 2013, **32**, 5136–5143.
- 13 (a) A. E. Cherian, J. M. Rose, E. B. Lobkovsky and G. W. Coates, *J. Am. Chem. Soc.*, 2005, **127**, 13770–13771; (b) J. M. Rose, A. E. Cherian and G. W. Coates, *J. Am. Chem. Soc.*, 2006, **128**, 4186–4187.
- 14 (a) D. H. Camacho and Z. Guan, *Macromolecules*, 2005, **38**, 2544–2546; (b) D. H. Camacho, E. V. Salo, J. W. Ziller and Z. Guan, *Angew. Chem., Int. Ed.*, 2004, **43**, 1821–1825.
- 15 (a) J. L. Rhinehart, L. A. Brown and B. K. Long, *J. Am. Chem. Soc.*, 2013, **135**, 16316–16319; (b) J. L. Rhinehart, N. E. Mitchell and B. K. Long, *ACS Catal.*, 2014, **4**, 2501–2504.
- 16 (a) S. Y. Dai, X. L. Sui and C. L. Chen, *Angew. Chem., Int. Ed.*, 2015, **54**, 9948–9953; (b) S. Y. Dai and C. L. Chen, *Angew. Chem., Int. Ed.*, 2016, **55**, 13281–13285.
- 17 (a) S. Y. Dai, S. X. Zhou, W. Zhang and C. L. Chen, *Macromolecules*, 2016, **49**, 8855–8862; (b) L. H. Guo, C. Zou, S. Y. Dai and C. L. Chen, *Polymers*, 2017, **9**, 122.
- 18 F. Z. Wang, J. C. Yuan, F. Y. Song, J. Li, Z. Jia and B. N. Yuan, *Appl. Organomet. Chem.*, 2013, **27**, 319–327.
- 19 (a) J. C. Jenkins and M. Brookhart, *Organometallics*, 2003, **22**, 250–256; (b) E. F. McCord, S. J. McLain, L. T. J. Nelson, S. D. Ittel, D. Tempel, C. M. Killian, L. K. Johnson and M. Brookhart, *Macromolecules*, 2007, **40**, 410–420.

